Structure−Activity Relationship of New Nonlinear Optical Organic Materials Based on Push−Pull Azo Dyes. 3. Guest−Host Systems

N. Tirelli* and U. W. Suter

Department of Materials, Institute for Polymers, ETH Zürich, Universitätstrasse 6, CH-8092 Zürich, Switzerland

A. Altomare, R. Solaro, and F. Ciardelli

Department of Chemistry and Industrial Chemistry, University of Pisa, via Risorgimento 35, 56126 Pisa, Italy

S. Follonier, Ch. Bosshard, and P. Günter

Department of Physics, Institute of Quantum Electronics, Nonlinear Optics Laboratory, ETH Zürich-Hönggerberg, CH-8093 Zürich, Switzerland

Received August 12, 1997; Revised Manuscript Received January 20, 1998

ABSTRACT: Several new push−pull azobenzene dyes with different electron-withdrawing groups, steric hindrance, and hydrogen-bonding capabilities were dispersed in poly(*N*-methacryloyl-*N*′-phenylpiperazine), a glassy polymer matrix. After orientation by corona poling, the second harmonic generation (SHG) signals of the guest−host systems were measured as a function of time and temperature and fitted with Kohlrausch−Williams−Watts (KWW) stretched exponentials. The variations of their nonlinear susceptibilities at time zero and in their relaxation behavior were correlated with the changes of the chromophore chemical structure. Rigid rod structures always presented the best orientability and stability of the nonlinear optical properties.

Introduction

In recent years, considerable research has been devoted to the study of the second-order nonlinear optical behavior of amorphous polymers,[1] due to their attractive potential applications in photonics.[2] In practice, one of the weak points of these materials is the need for an orientation procedure for the observation of phenomena such as second harmonic generation (SHG) and linear electrooptic effect: the orientability and the relaxation behavior of dipoles have to be respectively minimized and maximized to lead to applicable devices.

The study of the dipole behavior is easier when low molecular weight compounds are dispersed in a polymer matrix (guest−host systems) than for polymer-bound chromophores, taking advantage of the shorter time scale of the phenomena, the ease of synthesis, and the better chemical definition; in this way, guest−host systems can be used as models for the relaxation behavior of polymers.

Many efforts have been devoted to the study of orientation and randomization phenomena in glassy guest−host systems,[3−20] generally using second harmonic generation (SHG) as a tool for monitoring the growth and the decay of the organization of dipoles. However, to the best of our knowledge, no useful correlation among the chemical structure of NLO-active chromophores and their orientability and stability of second-order NLO properties has been yet presented.

In a previous paper[21] we reported the synthesis and molecular characterization of several new push−pull azobenzene chromophores with a rather continuous variation of structural features such as shape, hydrogen-bonding possibilities, and electronegativity of the electron-withdrawing group (Figure 1).

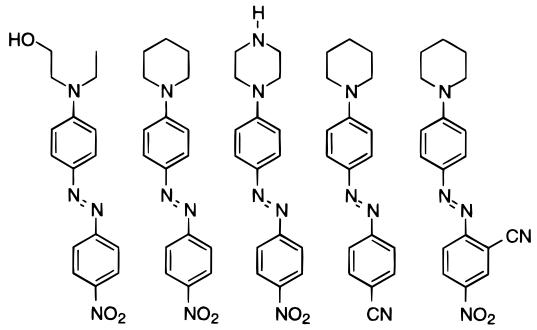

MOD 0 MOD 1 MOD 2 MOD 3 MOD 4

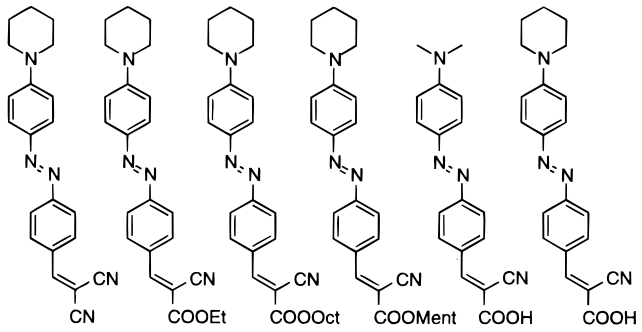

MOD 5 MOD 6 MOD 7 MOD8 MOD 9 MOD 10

Figure 1. Structures of azo dyes studied in this work.

In this paper, we have studied the influence of the chemical differences in these compounds on the NLO properties of guest−host systems obtained by dispersing the azo dyes in a polymer matrix. Disperse Red 1 (MOD 0), a well-known commercial dye, was used as a refer-

S0024-9297(97)01223-0 CCC: $15.00
Published on Web 03/13/1998

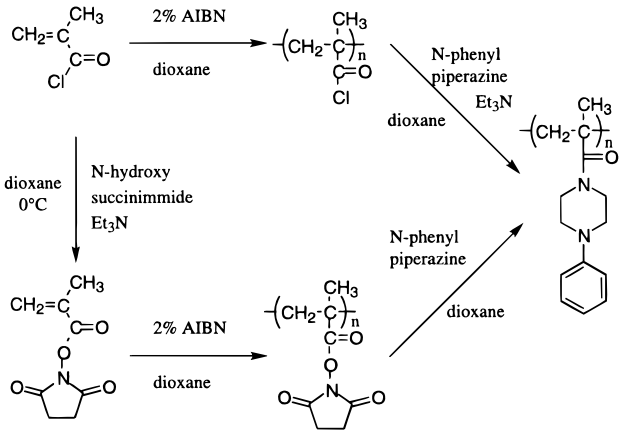

Figure 2. Scheme for the synthesis of PMPP.

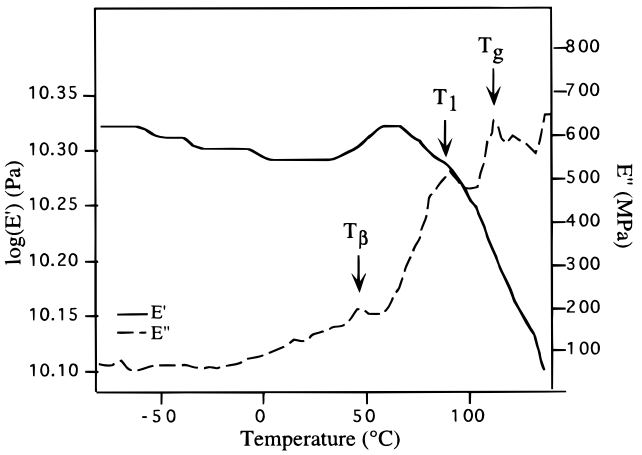

Figure 3. Storage and loss modulus temperature dependence for the system MOD 1/PMPP.

ence standard. Poly(*N*-methacryloyl-*N*′-phenylpiperazine) (PMPP) was chosen as the polymer host for the high structural similarity with the chromophores, to guarantee a good solubility and dispersability of the azo dyes.

Results and Discussion

Preparation and Characterization of Guest−Host Systems. The azobenzene derivatives were obtained by coupling of the diazonium salt of electron poor anilines with *N*,*N*-dialkylanilines, as already reported.[21]

Attempts to polymerize *N*-methacryloyl-*N*′-phenylpiperazine in the presence of either free-radical initiators, such as AIBN or BPO, or an anionic initiatior (*n*BuLi) failed. This behavior was not related to the dialkylaniline group: in fact, the *N*-methacryloyl-*N*′-phenylpiperazine hydrochloride was not able to polymerize in water or methanol solution by using potassium persulfate, alone or in mixture with sodium bisulfate, as a free-radical initiator.

Therefore, poly(*N*-methacryloyl-*N*′-phenylpiperazine) was prepared by a polymer-analogous reaction between a reactive prepolymer and *N*-phenylpiperazine (Figure 2). Poly(methacryloyl chloride) and poly(*N*-(methacryloyloxy)succinimide), both prepared by free-radical polymerization, were used.

Despite the advantages of *N*-(methacryloyloxy)succinimide, such as ease of use and larger stability of the polymer, the synthetic route starting from poly(methacryloyl chloride)[22] was preferred, for the almost quantitative conversion of the polymeric acyl chloride to the corresponding amide. On the contrary, complete substitution of the active ester groups was never achieved in the reaction of poly(*N*-(methacryloyloxy)succinimide).

The molecular weight of PMPP was evaluated from that of a poly(methyl methacrylate) sample obtained by reacting the reactive prepolymer with a mixture of sodium methoxide and methanol in THF, under the reasonable assumption that the functionalization reactions did not affect the degree of polymerization. The poly(MMA) sample showed an M_n of 53 000, corresponding to an average degree of polymerization of 530 and a polydispersity index (M_w/M_n) of 1.9. NMR analysis showed a 70% content of syndiotactic diads.

Thin films of the guest−host systems were prepared either by spin coating (for second harmonic generation and refractive index measurements) or by casting (for calorimetric measurements) 20% w/w solutions of the azobenzene chromophores and the polymer host in dry *N*-methylpyrrolidone (NMP). An 0.088:1 molar ratio between guest dye and polymer repeating units was used in all experiments.

DSC analysis revealed that the polymer T_g was lowered from 170 to 100−115 °C by the dispersion of the low molecular weight compounds; no melting transition was detected for either the pure polymer or the guest−host systems up to the decomposition temperature (over 250 °C).

The spin-coated films showed very good optical quality and transparency (89% of transmission at 750 nm exhibited by films spin coated on quartz slides); moreover, no sharp reflection was observed in X-ray diffractograms. This result and the absence of DSC transitions attributable to a phase separation are indicative of a good mixing of the dyes in the polymer matrix.

However, dynamic-mechanical thermal analysis (DMTA) (Figure 3) evidenced in all guest−host systems the presence of a transition, called transition 1, not detected by DSC, at about 15−25 deg below the T_g and above a β transition located between 30 and 50 °C.

The nature of this relaxation process is not clear; likely, it arises from a partial mobilization of the polymeric matrix close to the guest molecule, much less intense than that associated with the T_g: in fact, such a transition was not recorded for the pure polymer.

Nonlinear Optical Properties. The NLO inactivity of poly(*N*-methacryloyl-*N*′-phenylpiperazine) was confirmed by the absence of any SHG signal in thin polymer films under the same experimental conditions used for the guest−host systems.

The spin-coated films were oriented by corona poling: the procedure is described in the Experimental Section. After the poling field was switched off, the second harmonic signal time decay was recorded at eight different temperatures, i.e., 30, 70, 90, 100, 107, 114, 120, and 130 °C.

Due to the quick relaxation of the polar order, second-order nonlinear susceptibilities were measured at 30 °C, the Maker fringes experiments beginning 500 s after the end of the poling procedure, and then were extrapolated to time zero, using the previously studied reorientation kinetics at that temperature; in this way, the comparison between $\chi^{(2)}$ data is not affected by possible differences in relaxation rates.

Relaxation Experiments at 30 °C. The original intent of these experiments was to allow an extrapolation of the $\chi^{(2)}$ values at time zero, so they have been performed at the same temperature (30 °C), disregard-

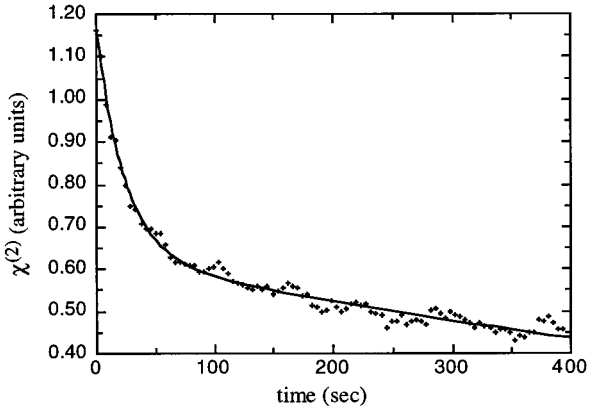

Figure 4. Experimental points and KWW fitting for the 120 °C SHG time decay for the system MOD 3/PMPP.

ing the temperature difference relative to T_g; this part of the study was intended to give essentially an overview of the materials performance, while a more accurate comparison of the relaxation behavior dependence on temperature will be presented in one of the next paragraphs.

The $\chi^{(2)}$ time decay at 30 °C presented an initial fast relaxation process, followed by a much slower one, as generally reported in the literature.[3,6,7,12−14,17,20] The experimental values of the second harmonic generation intensity (I_{SHG}) showed very good agreement (Figure 4) with a double exponential model, where the slow decay was fitted by a Kohlrausch−Williams−Watts (KWW) stretched exponential function:

$$\chi^{(2)}(t) = (I_{SHG})^{1/2} = A_1 \exp[-t/T_1] + A_2 \exp[-(t/\tau_2)^{b_2}]$$

The fast component could be easily fitted by either a KWW function or a simple exponential. Examples of both the former[3,6] and the latter procedure[7,16] can be found in the literature. The simple exponential fit was adopted in this case.

Our result for the faster decay rate constant (T_1) was about 10−20 s, independent of the temperature. This process has been attributed to the neutralization of surface charges; indeed, no similar process can be detected by contact electrode poling,[15] as well as by corona poling, if a surface discharge stage is used immediately after the poling process.[14]

Therefore, we focused our attention on the slower relaxation process, likely directly related to the dipole reorientation in the sample. To compare different guest−host systems, the average relaxation times $\langle\tau_2\rangle$ were calculated according to Lindsay and Patterson[23] and Wang:[12,24]

$$\langle\tau_2\rangle = \int_0^\infty \mathrm{d}t \exp\left[-(t/\tau_2)^{b_2}\right] = \frac{\tau_2}{b_2}\Gamma(b_2^{-1})$$

where Γ is the gamma function. This method takes proper account of the dispersion of relaxation times τ_2.

Comparing the $\langle\tau_2\rangle$ values, we highlighted a significant influence of the molecular structure of the guest chromophores (Table 1, Figure 5), while no linear correlation with the guest−host T_g values, reported in Table 2, was evident. In particular, the presence of 4-cyanovinyl groups and of alkyl chains greatly increased the orientational freedom to the chromophores.

Indeed, the relaxation rate decreased in going from MOD 0 (open structure) to MOD 1 (six-membered ring), from MOD 7 (long linear chain) to MOD 6 (short chain), to MOD 8 (menthyl ring), and to MOD 5 (no alkyl chain).

The introduction of groups able to form hydrogen bonds, such as carboxylic acids, primary alcohols, and secondary amines, did not significantly improve the stability of the polar order. In particular, acid functionalities seem to have a randomizing effect; this could be due to the likely higher ionic conductivity of these samples, which can lower the effective internal field during the poling.

MOD 3, the 4-cyano-substituted chromophore, showed the largest stability and one of the worst orientabilities (see next section); this behavior can be tentatively attributed to the formation of microaggregates within the host polymer matrix. This hypothesis is partially supported by the well-known tendency of cyano-substi-

Table 1. Orientability and Reorientation Properties for Guest−Host Systems

guest	$10^{-3}\langle\tau_2\rangle$ (s)[a]	d_{33} (pm/V)[a]	f_ω[b]	$f_{2\omega}$[b]	$10^{40}\beta^{1542nm}$ (m^2 V^2)[c]	order parameter (au)[d]
MOD 0	24.2	2.44	1.54	1.48	138	1.0
MOD 1	34.9	5.16	1.53	1.48	137	2.2
MOD 2	30.0	3.87	1.53	1.46	91	2.5
MOD 3	80.8	2.07	1.54	1.49	104	1.1
MOD 4	34.6	9.39	1.70	1.52	344	1.2
MOD 5	11.0	5.67	1.55	1.47	164	1.9
MOD 6	5.8	4.77	1.51	1.45	132	2.0
MOD 7	3.0	1.80	1.52	1.45	141	0.6
MOD 8	6.8	2.82	1.51	1.45	172	1.2
MOD 9	2.7	1.40	1.54	1.46	<130[e]	<0.6
MOD 10	3.1	0.94	1.53	1.46	<130[e]	<0.4

[a] Estimated error: 10%. [b] Estimated error: 2%. [c] Estimated error: <10%. [d] Estimated error: <25%. [e] No EFISH data available, value estimated to be slightly lower than that of MOD 6.

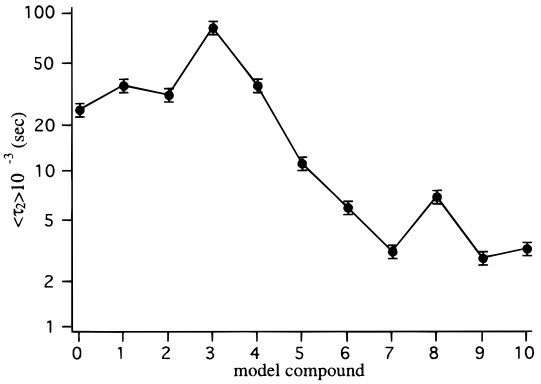

Figure 5. Average 30 °C relaxation times for the investigated guest−host systems. The line is just a guide for the eyes.

Table 2. Fitting Data for the Temperature Dependence of Relaxation Times

guest	$\tau_{\infty A}$[a] (s)	A[a] (K)	$\tau_{\infty V}$[b] (s)	B[b] (K)	T_0[b] (K)	T_x (°C)	T_1[c] (°C)	T_g[d] (°C)
MOD 0	85	1737	0.38	1586	200	84	93	115
MOD 1	0.64	3301	0.35	2144	139	83	89	112
MOD 2	203	1528	0.31	891	288	100	98	117
MOD 3	0.06	4250	0.25	1638	198	85	103	107
MOD 4	0.22	3625	3.18	632	282	98	95	106
MOD 5	0.29	3203	2.43	1181	190	97	88	122
MOD 6	2.65	2330	2.60	980	212	90	98	104
MOD 7	205	809	2.19	791	247	92	84	103
MOD 8	17.6	1824	1.98	899	241	99	99	108
MOD 9	0.95	2417	0.89	893	226	85	72	98
MOD 10	0.26	2820	0.80	812	251	103	100	127

[a] From Arrhenius fitting. [b] From VFT fitting. [c] By DMTA. [d] By DSC.

tuted aromatic compounds to form liquid crystalline phases. However, no evidence of aggregates could be obtained by optical, calorimetric, and X-ray diffraction measurements. On the other hand, no simple explanation of the significantly different behavior of MOD 3 as compared, for instance, with MOD 1 can be given on the basis of their rather small structural changes and dipole moment variations.[21]

Orientability of Chromophores. The chromophores orientational behavior can be better outlined by using an order parameter calculated from the nonlinear susceptibilities; in accordance with the oriented gas model, the second-order NLO coefficients can be expressed as

$$\chi_{33}^{(2)} = N\beta f_3^{2\omega}(f_3^{\omega})^2\langle\cos^3\theta\rangle$$

$$\chi_{31}^{(2)} = N\beta f_3^{2\omega}(f_1^{\omega})^2(\langle\cos\theta\rangle - \langle\cos^3\theta\rangle)/2$$

where N is the density of chromophores in the material, β is the main component of the hyperpolarizability tensor along the charge-transfer axis, f_ω and $f_{2\omega}$ are local field factors at the fundamental and second harmonic wavelength, and θ is the tilt angle between the chromophore molecular axis and the normal to the film.

β values at 1542 nm were computed from the corresponding measured values at 1907 nm with the electric field induced second harmonic generation (EFISH) technique,[21] by using the usual frequency dispersion law of the hyperpolarizability.[25] The local field factors were calculated according to the Lorentz model;[5] the refractive index dispersion data were measured on not-poled thin films, spin coated on quartz slides, assuming the polymer to be not birefringent, and consequently, $f_1^{\omega} = f_3^{\omega}$. For the sake of simplicity, the ratio d_{33}/d_{31} was assumed to be equal to 3.[26] The $\langle\cos^3\theta\rangle$ values were used as order parameters.

The chromophore volume density, even if kept constant in all the samples, was not determined; therefore, the order parameters were evaluated relative to that of the MOD 0 dispersion, used as a standard.

The order parameter used in the present work is analogous to the polar orientational order parameters (POP) calculated by Wang et al.;[5] these coefficients have been recognized to be strongly dependent on concentration. Therefore, a quantitative comparison between different chromophores can be made only under the assumption that the concentration dependence of POP is the same for all the guest−host systems; this assumption should hold for the investigated molecules, due to their structural similarity.

The values of the second-order nonlinear optical susceptibilities, expressed as d_{33}, are reported in Table 1 together with the data for f_ω and $f_{2\omega}$, for $\beta^{1542\text{nm}}$, and for the order parameter, expressed as

$$\frac{\langle\cos^3\theta\rangle}{(\langle\cos^3\theta\rangle)_{\text{MOD0}}}$$

In Figure 6 the second-order susceptibility and order parameter data are summarized.

Comparison of the order parameters indicates generally that rigid rod structures are the most orientable, whereas alkyl chains not only cause a quicker relaxation, but also decrease the orientability. Carboxylic acid groups exhibit the same effect to a greater extent.

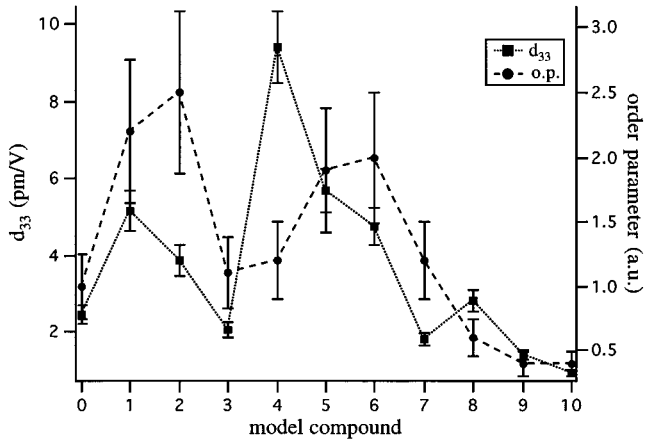

Figure 6. Second-order nonlinear susceptibilities (d_{33}) and order parameters for the investigated guest−host systems. Dotted and dashed lines are just guides for the eyes.

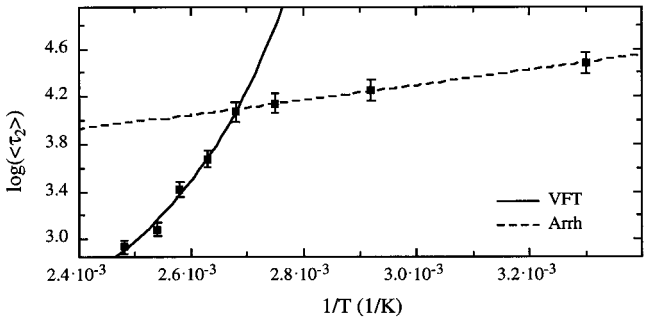

Figure 7. Experimental points, Arrhenius (Arrh) and Vogel−Fulcher−Tammann (VFT) fittings for the temperature dependence of average relaxation times in the system MOD 2/PMPP.

The orientations and relaxation behaviors of MOD 1 and MOD 2 are very similar: no significant effect of secondary amine was visible, except in the decrease of the d_{33} value. This finding can be attributed to the formation of an intramolecular hydrogen bond by the N−H group,[21] which lowers the hyperpolarizability while not appreciably influencing the molecular stiffness.

MOD 4 showed a very low orientability, possibly because of both the deviation from the rodlike shape and the lower dipole moment value;[21] in any case, its exceptional β value allowed the MOD 4 polymer dispersion to exhibit the highest d_{33}.

Relaxation Experiments at Different Temperatures. All investigated guest−host systems exhibited a singularity in the plot of $\langle\tau_2\rangle$ vs temperature, globally showing a non-Arrhenius-type behavior.

Accordingly with the literature, Arrhenius[27,28] and nonexponential fits (such as Williams−Landel−Ferry or Vogel−Fulcher−Tammann (VFT) equations)[7,28,29,30] are used respectively for fitting the relaxation times at temperatures below and above the T_g (Figure 7); in this case we have used the VFT fit, being given by[31]

$$\tau(T) = \tau_{\infty V}\exp(B/(T - T_0))$$

where $\tau_{\infty V}$ is the high-temperature asymptotic relaxation time, B is an apparent activation temperature, and T_0 is sometimes seen as an asymptotic value for T_g in the limit of reversible cooling.[31]

A very good fit was observed, but the small number of experimental points did not allow us to assess whether a real nonexponential behavior or simply a

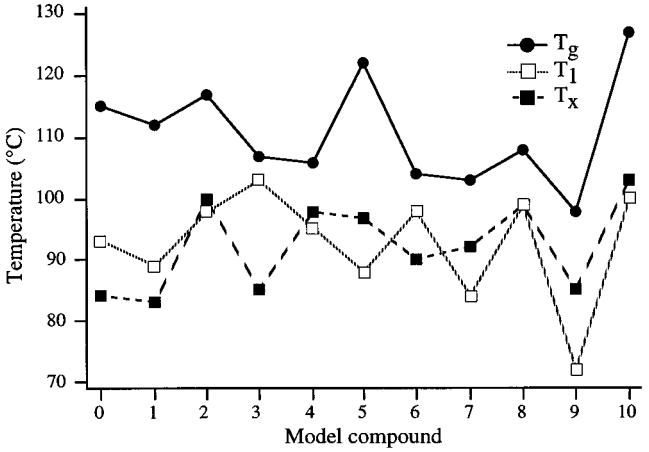

Figure 8. T_g, T_x, and T_1 values for the investigated guest−host systems. Solid, dashed, and dotted lines are just guides for the eyes.

different Arrhenius dependence, as suggested by Schüssler et al.,[15] was present above T_g.

The fitting parameters are reported in Table 2 only for qualitative purposes, due to the limited number of data. It is, however, possible to highlight some regularities, such as the decrease in the activation temperature A and the increase in asymptotic relaxation time $\tau_{\infty A}$ on increasing the conformational mobility in the series MOD 5, MOD 6, MOD 8, and MOD 7; in the VFT fitting region, these differences are greatly reduced, as expected from the much larger mobility of the rubbery matrix.

Interestingly, the crossing of the two fittings always occurred at a temperature (T_x) 15−25 deg below the T_g value evaluated by DSC analysis, in the same temperature range where DMTA analysis evidenced the presence of transition 1 (T_1).

The comparison of T_1 and T_x values suggests a likely identification of the two temperatures. The agreement between the two sets of data is acceptably good, with the only possible exception of MOD 3, taking into account the different nature of the measurement techniques and the poor accuracy of the T_x detection (Figure 8).

This hypothesis, if confirmed, indicates that the relaxation behavior of these guest−host systems does not directly depend on T_g and that appreciable chromophore movements occur well before complete mobilization of the polymer main chain. Dielectric relaxation experiments were performed, but unfortunately they did not give any help in understanding the phenomenon: in all cases the guest−host films showed a too high conductivity at that temperature to allow the fine determination of sub-T_g transitions.

This phenomenon should be carefully investigated for chromophore dispersions, particularly when the operating temperature is not far from T_g.

Photoorientation Experiments. Push−pull azobenzene dyes are known to photoisomerize to the cis form under irradiation in the 400−500 nm absorption band and to back-isomerize very quickly to the trans form even at room temperature. This photochemical process has been sometimes used to mobilize the chromophores, thus easing the electric poling, at temperatures lower than T_g.[32]

An excitation wavelength of 488 nm (Ar laser, 0.05 W/cm^2) was chosen, the absorption from the cis isomers being negligible in that spectral zone.[33] Experiments of solid-state photoisomerization were performed at room temperature with the poling field on, above T_g with the poling field on, and at room temperature, after a complete poling procedure, with the poling field off.

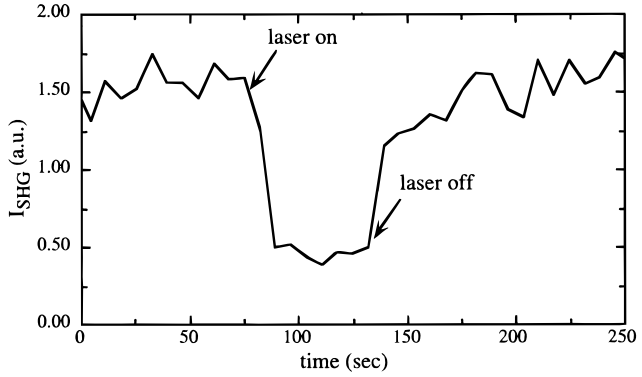

Figure 9. SHG intensity with and without 488 nm irradiation at 125 °C for the system MOD 6/PMPP under the poling field.

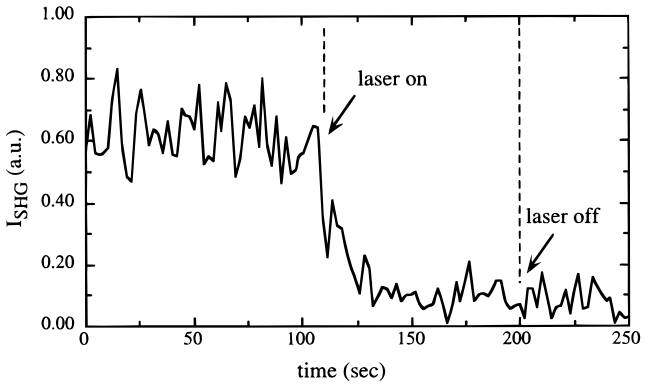

Figure 10. SHG intensity with and without 488 nm irradiation at 30 °C for the system MOD 6/PMPP (time 0 corresponds to 600 s after switching off the poling field).

The first two sets of experiments afforded similar results: the SHG level dropped to zero during the irradiation period, the chromophore orientation being randomized as an effect of the photoisomerization processes, and then returned to the original value with no appreciable improvement (Figure 9).

When the irradiation was carried out on a poled sample, the photoisomerization reaction very rapidly erased the polar order in the material and any SHG signal (Figure 10). This procedure may constitute a powerful tool to write an NLO-active pattern in the polymer film, potentially with a very high resolution.

All the investigated chromophores showed similar randomization time constants, estimated in 1−5 s^{-1} assuming a single exponential behavior; however, the low signal-to-noise ratio of the Raman cell used for the SHG did not allow a precise determination of them.

Experimental Section

Materials. 2-Cyanoacetic acid, *N*-methylpyrrolidinone (NMP), *N*,*N*-dimethylaniline, *N*-phenylpiperidine, and *N*-phenylpiperazine were distilled under reduced pressure, respectively, at 103 °C/0.05 mmHg, 40 °C/1 mmHg on CaH_2, 30 °C/0.3 mmHg on KOH, 97/0.7 mmHg on KOH, and 125 °C/7 mmHg on KOH. Triethylamine was distilled at 88 °C on $LiAlH_4$. Methacryloyl chloride was distilled at 100 °C on quinoline. Dioxane was refluxed and distilled on Na/K alloy. 2,2′-Azobis(isobutyronitrile) (AIBN) and benzoyl peroxide (BPO) were recrystallized from ethanol. MOD 0 (Disperse Red 1,

Aldrich) was recrystallized from dioxane. The other reagents were obtained from Aldrich Chemicals or Fluka and used as received.

The synthesis of all the chromophores, except MOD 0, MOD 9, and MOD 10, has already been published elsewhere.[21]

***p*-Amino-α-Cyanocinnamic Acid.** To a solution of 6.4 g (53 mmol) of *p*-aminobenzaldehyde and 4.5 g (53 mmol) of 2-cyanoacetic acid in 150 mL of dioxane was added 0.8 mL of a catalyst, obtained from 0.2 mL (3.2 mmol) of piperidine and 0.6 mL of acetic acid. The mixture was refluxed for 10 h, then cooled to 0 °C, and filtered; the collected powder was suspended in 150 mL of CH_2Cl_2 and treated with 300 mL of 10% $NaHCO_3$, stirring the system till disappearance of any residual solid. The aqueous phase was brought to pH = 4 with 10% HCl and filtered to give a moist yellow paste; after azeotropic benzene distillation, 5.4 g (yield 54%) of yellow powder was isolated. Mp = 223 °C. ^{1}H NMR (DMSO-d_6): δ = 13.5−12.5 (1H, COO*H*), 8.0 (s, 1H, C*H*═C), 7.8−7.9 (d, 2H, aromatic C*H* in position meta to NH_2), 6.8−6.3 ppm (d + t, 4H, aromatic C*H* in position ortho to NH_2 and NH_2). FT-IR (KBr pellet): ν = 3465 and 3365 (N−H stretching), 3090 (aromatic C−H stretching), 3000−2000 (O−H stretching), 2223 (nitrilic CN stretching), 1668 (C═O stretching), 1630 (NH_2 bending), 1609 (C═C stretching), 1570 and 1514 (aromatic ring vibrations), 1327 (aniline C−N stretching), 1286 and 1236 (asymmetric and symmetric C−O−C stretching), 1177 and 830 cm^{-1} (in-plane and out-of-plane bending of aromatic protons). UV−vis (chloroform): λ_{max} = 385 nm, ϵ = 33 500 mol^{-1} cm^{-1}.

4-(2-Cyano-2-carboxyvinyl)-4′-(*N*-dimethylamino)azobenzene (MOD 9). *p*-Amino-α-cyanocinnamic acid (2.6 g, 14 mmol) was dissolved in 100 mL of 10% $NaHCO_3$. The solution was then cooled to 5 °C, and acetic acid was added till acidity; a fine suspension was obtained, to which 1.0 g (14 mmol) of $NaNO_2$ dissolved in 3 mL of water was slowly added. All the suspended material dissolved, and the color turned to light orange. The solution was warmed to room temperature and stirred for 30 min; then the temperature was lowered to 7−8 °C and 1.7 g (14 mmol) of *N*,*N*-dimethylaniline dissolved in 10 mL of acetic acid was added. The color turned to red-violet. The solution was warmed to room temperature and stirred for 5 h; then, after the addition of 300 mL of water, a violet solid precipitated. This was filtered, anhydrified with azeotropic benzene distillation, and recrystallized from dioxane. Dark red crystals (3.6 g, 80% yield) were obtained. No melting point before decomposition (T > 265 °C). ^{1}H NMR (DMSO-d_6): δ = 9−10 (1H, COO*H*), 8.3 (s, 1H, C*H*═C), 8.1 (d, 2H, aromatic C*H* ortho to vinyl group), 7.8 (m, 4H, aromatic C*H* meta to vinyl group and meta to aniline), 6.85 (d, 2H, aromatic C*H* ortho to aniline), 3.1 ppm (s, 4H, N−CH_3). FT-IR (KBr pellet): ν = 3100−3000 (aromatic C−H stretching), 2915−2900 (aliphatic C−H stretching), 2224 (nitrilic CN stretching), 1698 (C═O stretching), 1602 and 1519 (aromatic ring vibrations), 1362 (aniline aromatic C−N stretching), 1233 (aniline aliphatic C−N stretching), 845 and 823 cm^{-1} (out-of-plane bending of aromatic protons). UV−vis (chloroform): λ_1 = 484 nm, ϵ = 29 600 mol^{-1} cm^{-1}; λ_2 = 323 nm, ϵ = 13 600 mol^{-1} cm^{-1}.

4-(2-Cyano-2-carboxyvinyl)-4′-(*N*-piperidinyl)azobenzene (MOD 10). The procedure reported for MOD 9 was repeated by using *N*,*N*-dimethylaniline instead of *N*-phenylpiperazine, to give 72% of dark red crystals, having mp = 272 °C. ^{1}H NMR (DMSO-d_6): δ = 9−10 (1H, COO*H*), 8.3 (s, 1H, C*H*═C), 8.1 (d, 2H, aromatic C*H* ortho to vinyl group), 7.8 (m, 4H, aromatic C*H* meta to vinyl group and meta to aniline), 6.85 (d, 2H, aromatic C*H* ortho to aniline), 3.45 (s, 4H, N−CH_2−CH$_2$), 1.7 ppm (s, 6H, N−CH$_2$−CH_2−CH_2−CH_2−CH$_2$−N). FT-IR (KBr pellet): ν = 3100−3000 (aromatic C−H stretching), 2930−2860 (aliphatic C−H stretching), 2218 (nitrilic CN stretching), 1698 (C═O stretching), 1593 and 1509 (aromatic ring vibrations), 1358 (aniline aromatic C−N stretching), 1240 (aniline aliphatic C−N stretching), 840 and 821 cm^{-1} (out-of-plane bending of aromatic protons). UV−vis (chloroform): λ_1 = 486 nm, ϵ = 30 800 mol^{-1} cm^{-1}; λ_2 = 325 nm, ϵ = 14 800 mol^{-1} cm^{-1}.

Poly(methacryloyl chloride). Into a Schlenk tube under a dry nitrogen atmosphere were distilled 25 mL (0.25 mol) of methacryloyl chloride and 55 mL of dry dioxane; 0.86 mL (5 mmol) of AIBN was then added, and the solution was degassed under vacuum at the liquid nitrogen temperature and then heated at 60 °C for 44 h. Always under a dry nitrogen atmosphere, the solution was poured into 600 mL of freshly distilled (on $LiAlH_4$) hexane; the solid was collected on a glass filter and washed twice with hexane. A white powder (24.4 g, 89.1% yield) was obtained after vacuum-drying. ^{1}H NMR ($CDCl_3$): δ = 2.25 (CH_2), 1.25 ppm (CH_3). FT-IR (KBr pellet): ν = 2950−2850 (aliphatic C−H stretching), 1783 (C═O stretching), 1470 (CH_2 scissoring), 1445 and 1380 (asymmetric and symmetric CH_3 bending), 845 cm^{-1} (C−Cl stretching).

***N*-(Methacryloyloxy)succinimide.** To a solution of 11.5 g (0.100 mol) of *N*-hydroxysuccinimide, 14.4 mL (0.200 mol) of triethylamine, and 10 mg of 2,6-di-*tert*-butyl-*p*-cresol in 100 mL of dry dioxane were slowly added at 0 °C under a dry nitrogen atmosphere 14.5 mL (0.150 mol) of methacryloyl chloride dissolved in 20 mL of dry dioxane.

The mixture was stirred at 0 °C for 1 h and then allowed to stand at room temperature for 16 h. After evaporation of the solvent, the solid was dissolved in methylene chloride and the solution was washed with HCl 5%, $NaHCO_3$ 10%, and water till neutrality, then dried on Na_2SO_4, and evaporated. After crystallization from ethanol/hexane, 13.4 g (73% yield) of white crystals was obtained. ^{1}H NMR ($CDCl_3$): δ = 6.3 (s, 1H, C*H*H═C in position cis to the ester), 5.8 (s, 1H, C*H*H═C in position trans to the ester), 2.75 (s, 4H, CH_2 in the ring), 1.95 ppm (s, 3H, ═CCH_3). FT-IR (KBr pellet): ν = 3085 (vinylic C−H stretching), 2930−2850 (aliphatic C−H stretching), 1800−1659 (esteric C═O and C═C stretching), 1635 (amidic C═O stretching), 1200 and 1095 cm^{-1} (asymmetric and symmetric C−O−C stretching).

Poly(*N*-(methacryloyloxy)succinimide). *N*-(methacryloyloxy)succinimide (5 g, 0.027 mol) and 90 mg of AIBN, dissolved in 20 mL of dry dioxane were introduced in a glass vial under a nitrogen atmosphere; the vial was degassed at the liquid nitrogen temperature, sealed under high vacuum, and then heated at 60 °C for 44 h. The reaction mixture was precipitated in 300 mL of hexane, and the so obtained solid was dissolved in dioxane and reprecipitated in hexane. A white powder (4.7 g, 94% yield) was obtained after vacuum-drying. FT-IR (KBr pellet): ν = 3500−2500 (O−H stretching), 2930−2850 (aliphatic C−H stretching), 1800−1659 (esteric + acid C═O stretching), 1635 (amidic C═O stretching), 1200 and 1110 (asymmetric and symmetric C−O−C stretching), 1040 cm^{-1} (C−C stretching or chains vibrations).

Poly(*N*-methacryloyl-*N*′-phenylpiperazine) from Poly(methacryloyl chloride). Poly(methacryloyl chloride) (21.5 g, 0.20 equiv) was dispersed in 600 mL of in situ distilled dioxane; after 3 h the dissolution was complete, and 57 mL (0.40 mol) of triethylamine and 33 mL (0.22 mol) of *N*-phenylpiperazine, both freshly distilled, were dropwise added. After 4 h at room temperature, the solution was warmed to 60 °C with stirring for 24 h. After cooling, the reaction mixture was concentrated and precipitated in 700 mL of methanol and the so obtained solid was dissolved in methylene chloride and reprecipitated in methanol. White powder (26.7 g, 58% yield) was obtained after vacuum-drying. T_g = 170 °C. ^{1}H NMR ($CDCl_3$): δ = 7.15 (2H, aromatic C*H* in position meta to the nitrogen), 6.7 (3H, aromatic C*H* in positions ortho and para to the nitrogen), 4.2−0.7 ppm (13 H, aliphatic protons). FT-IR (KBr pellet): ν = 3100−3000 (aromatic C−H stretching), 2970−2840 (aliphatic C−H stretching), 1625 (C═O stretching), 1600 and 1503 (aromatic ring vibrations), 1230 (aliphatic amidic C−N stretching), 1180 (aliphatic anilinic C−N stretching), 865 cm^{-1} (aromatic protons out-of-plane bending).

Physicochemical Measurements. IR spectra were recorded by a Nicolet 5SXC FT-IR spectrometer on KBr pellets. UV spectra were recorded by a Perkin-Elmer Lambda 9 spectrometer. ^{1}H NMR spectra were recorded on a Bruker 300 MHz spectrometer on $CDCl_3$ solutions; tetramethylsilane (TMS) was used as an internal standard. DSC analysis was performed under a nitrogen atmosphere at a heating rate of 10 °C/min by a Mettler TA 4000 calorimeter, equipped with a DSC 30 low-temperature cell. DMTA was performed at a

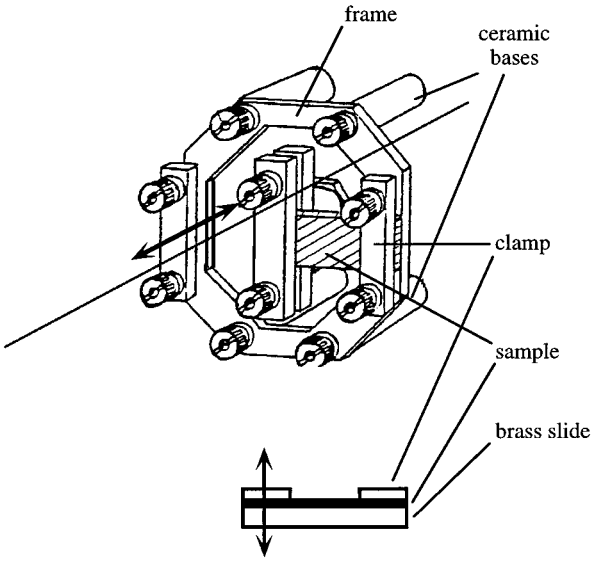

Figure 11. Bending mode DMTA setup. The movement direction is represented by the double arrow.

heating rate of 2 °C/min, a frequency of 1 Hz, and a deformation of 0.1 mm by a Polymer Laboratories Thermal Analysis dynamic-mechanical analyzer working in the bending mode (sketched in Figure 11) and equipped with a low-temperature cell.

Film Preparation. Appropriate amounts of chromophore and PMPP (molar ratio between dye and monomeric unit: 0.088) were dissolved in freshly distilled NMP to give 20% w/w solutions; after filtration (Teflon filter with porosity of 0.45 μm), the films were prepared by spin coating ITO-coated glass slides for SHG measurements or quartz slides for refractive index measurements. The films were placed in a vacuum oven at 80 °C for 3 days in order to remove any residual solvent; the film thickness was measured with a profilometer Alphastep.

Films were also prepared by solution casting on brass slides, for bending mode DMTA, or on glass slides, for preparation of DSC samples.

The X-ray diffraction experiments were performed on thin films in reflection mode with a Siemens Kristalloflex diffractometer.

Optical Measurements. The refractive indices of the thin films were measured on quartz slides using transmission spectroscopy and describing the real part of the refractive index with a Sellmeyer-type dispersion formula.[34,35]

The second harmonic generation experimental setup is described in detail elsewhere described;[36] it involved a Q-switched Surelite Nd:YAG laser ($\lambda = 1.064$ μm, frequency up to 10 Hz, 8.5 mJ/pulse), pumping a methane Raman cell with output at 1.542 μm. The beam intensity was measured by performing a Maker fringes reference experiment with a quartz crystal (110) ($d_{11} = 0.4$ pm/V[37]). The sample holder was mounted on a computer-controlled goniometer stage with the possibility of temperature control to $\pm$0.1 deg. The corona poling techinque was used to orient the dipoles, using a 6.5 kV potential difference between the needle and the sample, placed at a costant distance of 2 cm. The poling experiments were performed by measuring the SHG growth at a fixed angle (35°), with the following temperature profile: heating to 130 °C; 30 min isotherm; cooling to 90 °C at 1 deg/min; 30 min isotherm; cooling to room temperature at 1 deg/min. The 90 °C annealing was performed only for relaxation experiments at room temperature.

Summary and Conclusions

In this study we have presented the preparation of several guest−host systems and a study of their nonlinear optical properties based on the second harmonic generation of corona poling oriented samples; we have investigated the chemical structure dependence of the orientability achieved with electric poling and of the orientation stability. The orientability has been studied using an order parameter proportional to $\langle \cos^3 \theta \rangle$ and normalized to the orientability of a commercial chromophore (MOD 0).

We have demonstrated that rigid rod chromophores are always better oriented and randomize slower than analogous compounds with more degrees of conformational freedom. Alkyl chains decrease the orientability and the stability with increasing flexibility and length. Acid groups act as powerful randomizing agents. Other potentially hydrogen-bonding groups, like primary alcohol or secondary amine, do not show any remarkable effect for the polar order stabilization.

The chromophore bearing the cyano group as the electron-withdrawing substituent shows a straightforward stability, together with a surprisingly low (for the rigid rod structure) orientability; this result has been tentatively attributed to some sort of aggregation phenomena.

Despite its poor orientability, the chromophore MOD 4, bearing two noncollinear electron-withdrawing groups, shows the highest d_{33} values because of the very high molecular hyperpolarizability. A good way to improve the chromophore structure should probably be to expand its molecular length, to increase the dipole moment and rodlike shape.

Finally, we have analyzed the temperature dependence of the relaxation processes. The critical temperature for the change to a non-Arrhenius behavior does not correspond to the glass transition as detected by DSC and DMT analyses, but where DMTA allocated a first sub-T_g transition. Separate dielectric measurements did not help to interpret the phenomenon, due to the too high conductivities of the samples, but confirmed a more mobile state of the system at that temperature.

The nature of this process is not yet clear, but it has been tentatively explained as a mobilization of the local chromophore environment from a glassy to a fluid state, not involving directly, however, the polymer main chains.

Acknowledgment. We thank Remy Stoll for the technical advice in performing DMTA analyses and Peter Neuenschwander for helpful discussions. Financial support from the D4 COST project and from the Swiss National Science Foundation is gratefully acknowledged.

References and Notes

(1) *Polymers for Nonlinar Optics*; Lindsay, G. A., Singer, K. D., Eds.; American Chemical Society: Washington, DC, 1995.
(2) Dagani, R. *Chem. Eng. News* **1996**, March 4.
(3) Hampsch, H. L.; Yang, J.; Wong, G. K.; Torkelson, J. M. *Macromlecules* **1990**, *23*, 3640.
(4) Wang, C. H. *J. Chem. Phys.* **1993**, *98*, 3457.
(5) Guan, H. W.; Wang, C. H. *J. Chem. Phys.* **1993**, *98*, 3463.
(6) Wang, C. H.; Gu, S. H.; Guan, H. W. *J. Chem. Phys.* **1993**, *99*, 5597.
(7) Goodson, T.; Wang, C. H. *Macromolecules* **1993**, *26*, 1837.
(8) Walsh, C. A.; Burland, D. M.; Lee, V. Y.; Miller, R. D.; Smith, B. A.; Twieg, R. J.; Volksen, W. *Macromolecules* **1993**, *26*, 3720.
(9) Dhinojwala, A.; Wong, G. K.; Torkelson, J. M. *Macromolecules* **1993**, *26*, 5943.
(10) Dhinojwala, A.; Hooker, J. C.; Torkelson, J. M. *J. Non-Cryst. Solids* **1994**, *172−174*, 286.

(11) Dhinojwala, A.; Wong, G. K.; Torkelson, J. M. *J. Opt. Soc. Am. B* **1994**, *11*, 1549.
(12) Guan, H. W.; Pauley, M. A.; Brett, T.; Wang, C. H. *J. Polym. Sci. B: Polym. Phys. Ed.* **1994**, *32*, 2615.
(13) Goodson, T.; Gong, S. S.; Wang, C. H. *Macromolecules* **1994**, *27*, 4278.
(14) Wang, H.; Jarnagin, R. C.; Samulski, E. T. *Macromolecules* **1994**, *27*, 4705.
(15) Schüssler, S.; Richert, R.; Bässler, H. *Macromolecules* **1994**, *27*, 4318.
(16) Dirk, C. W.; Devanathan, S.; Velez, M. *Macromolecules* **1994**, *27*, 6167.
(17) Brower, S. C.; Hayden, L. M. *J. Polym. Sci. B: Polym. Phys. Ed.* **1995**, *33*, 2391.
(18) Schüssler, S.; Richert, R.; Bässler, H. *Macromolecules* **1995**, *28*, 2429.
(19) Pauley, M. A.; Wang, C. H.; Jen, A. K. Y. *Macromolecules* **1996**, *29*, 7064.
(20) Man, H. T.; Yoon, H. N. *Adv. Mater.* **1992**, *4*, 159.
(21) Tirelli, N.; Solaro, R.; Altomare, A.; Ciardelli, F.; Meier, U.; Bosshard, C.; Günter, P. *J. Prakt. Chem.*, in press.
(22) Strohriegl, P. *Makromol. Chem.* **1993**, *194*, 363.
(23) Lindsey, C. P.; Patterson, G. D. *J. Chem. Phys.* **1980**, *73*, 3348.
(24) Wang, C. H.; Fytas, G.; Lilge, D.; Dorfmüller, T. H. *Macromolecules* **1981**, *14*, 1363.
(25) Oudar, J. L.; Chemla, D. S. *J. Chem. Phys.*, **1977**, *66* (6), 2664.
(26) Bosshard, Ch.; Sutter, K.; Pretre, Ph.; Hulliger, J.; Flörsheimer, M.; Kaatz, P.; Günter, P. *Organic Nonliear Optical Materials. Adv. Nonlinear Opt.* **1996**, *1*, 94.
(27) Singer, K. D.; King, L. A. *Polym. Prepr. (Am. Chem. Soc., Div. Polym. Chem.)* **1991**, *32*, 198.
(28) Dhinojwala, A.; Wong, G. K.; Torkelson, J. M. *J. Chem. Phys.* **1994**, *100*, 6046.
(29) Stähelin, M.; Burland, D. M.; Ebert, M.; Miller, R. D.; Smith, B. A.; Twieg, R. J.; Volksen, W.; Walsh, C. A. *Appl. Phys. Lett.* **1992**, *61*, 1626.
(30) Stähelin, M.; Walsh, C. A.; Burland, D. M.; Miller, R. D.; Twieg, R. J.; Volksen, W. *J. Appl. Phys.* **1993**, *73*, 8471.
(31) Ferry, J. D. *Viscoelastic Properties of Polymers*; Wiley; New York, 1990.
(32) Blabchard, P. M.; Mitchell, G. R. *J. Phys. D: Appl. Phys.* **1993,** *26*, 500.
(33) Wildes, P. D.; Pacifici, J. G.; Irick, G.; Whitten, D. G. *J. Am. Chem. Soc.* **1971**, *93*, 2004.
(34) Magnificier, J. C.; Gasiot, J.; Fillard, J. P. *J. Phys. E: Sci. Instrum.* **1983**, *16*, 1002.
(35) Bosshard, Ch. Doctoral Thesis at the Swiss Federal Institute of Technology, Zurich, Switzerland, Diss. n. 9407, 1991.
(36) Weder, C.; Neuenschwander, P.; Suter, U. W.; Prêtre, P.; Kaatz, P. Günter, P., *Macromolecules* **1994**, *27*, 2181.
(37) Landolt-Börnstein. In *Elastische, piezoelektrische, pyroelektrische, piezooptische Knostanten und nichtlineare dielektrische Suszeptibilitäten von Kristallen*; Hellwege, K. H., Hellwege, A. M., Eds.; Springer-Verlag: Berlin, 1979; Vol. II, p 11.

MA971223L